Biogeosciences Discuss., 11, 2569–2593, 2014
www.biogeosciences-discuss.net/11/2569/2014/
doi:10.5194/bgd-11-2569-2014

Biogeosciences
Discussions
Open Access

Climate vs. carbon dioxide controls on biomass burning: a model analysis of the glacial-interglacial contrast

M. Martin Calvo[1], I. C. Prentice[2,3], and S. P. Harrison[3,4]

[1]Department of Life Sciences, Imperial College London, Silwood Park, Buckhurst Road, Ascot SL5 7PY, UK
[2]AXA Chair of Biosphere and Climate Impacts, Grantham Institute for Climate Change and Grand Challenges in Ecosystems and the Environment, Department of Life Sciences, Imperial College London, Silwood Park, Buckhurst Road, Ascot SL5 7PY, UK
[3]Department of Biological Sciences, Macquarie University, Sydney, North Ryde, NSW 2109, Australia
[4]Centre for Past Climate Change and School of Archaeology, Geography and Environmental Sciences (SAGES), University of Reading, Whiteknights, RG6 6AH, Reading, UK

Received: 7 January 2014 – Accepted: 15 January 2014 – Published: 12 February 2014

Correspondence to: M. Martin Calvo (m.martin-calvo@imperial.ac.uk)

Published by Copernicus Publications on behalf of the European Geosciences Union.

Abstract

Climate controls fire regimes through its influence on the amount and types of fuel present and their dryness; CO_2 availability, in turn, constrains primary production by limiting photosynthetic activity in plants. However, although fuel accumulation depends on biomass production, and hence CO_2 availability, the links between atmospheric CO_2 and biomass burning are not well known. Here a fire-enabled dynamic global vegetation model (the Land surface Processes and eXchanges model, LPX) is used to attribute glacial-interglacial changes in biomass burning to CO_2 increase, which would be expected to increase primary production and therefore fuel loads even in the absence of climate change, vs. climate change effects. Four general circulation models provided Last Glacial Maximum (LGM) climate anomalies – that is, differences from the pre-industrial (PI) control climate – from the Palaeoclimate Modelling Intercomparison Project Phase 2, allowing the construction of four scenarios for LGM climate. Modelled carbon fluxes in biomass burning were corrected for the model's observed biases in contemporary biome-average values. With LGM climate and low CO_2 (185 ppm) effects included, the modelled global flux was 70 to 80 % lower at the LGM than in PI time. LGM climate with pre-industrial CO_2 (280 ppm) however yielded unrealistic results, with global and Northern Hemisphere biomass burning fluxes greater than in the pre-industrial climate. Using the PI CO_2 concentration increased the modelled LGM biomass burning fluxes for all climate models and latitudinal bands to between four and ten times their values under LGM CO_2 concentration. It is inferred that a substantial part of the increase in biomass burning after the LGM must be attributed to the effect of increasing CO_2 concentration on productivity and fuel load. Today, by analogy, both rising CO_2 and global warming must be considered as risk factors for increasing biomass burning. Both effects need to be included in models to project future fire risks.

1 Introduction

Burnt area, the primary aspect of biomass burning that is most relevant to the carbon cycle since it determines carbon fluxes to the atmosphere (Prentice et al., 2011a), is controlled primarily by fuel availability and secondly by fuel dryness (Krawchuk et al., 2009; Krawchuk and Moritz, 2009, 2011; Aldersley et al., 2011; Moritz et al., 2013; Bistinas et al., 2013). Both of these are influenced by climate: short-term stochastic climate variability (weather) controls ignitions and fuel moisture and hence fire starts and fire spread; long-term climate controls vegetation type and productivity, and hence fuel production (Dale et al., 2000; Flannigan et al., 2000; Bowman et al., 2009; Harrison et al., 2010). However, vegetation type and productivity are also directly and independently influenced by atmospheric CO_2 levels (Farquhar, 1997; Cowling, 1999; Prentice and Harrison, 2009). This opens up the possibility that changes in atmospheric CO_2 levels, for example over the 20th and 21st centuries as a consequence of human activities (Denman et al., 2007), could have an impact on biomass burning (Koch and Mooney, 1996; Moritz et al., 2005; Harrison et al., 2010).

Progress in differentiating between these large-scale controls of fire could be made by evaluating changes in fire regimes with the help of global vegetation-fire models that (a) represent the controlling processes and their interactions mechanistically, and (b) have been shown to reproduce major spatial and temporal patterns in fire regimes as observed from space. However, direct observations of changes in global biomass burning are too short to discriminate between climate and direct CO_2 effects on fire regimes: the most reliable remotely-sensed record of burnt area is derived from MODIS, which started in 2000 CE (Giglio et al., 2010). Thus an alternative approach is required to evaluate whether changes in CO_2 could significantly influence biomass burning, making using of palaeodata that document the response of fire regimes to climate changes on geologic timescales.

Sedimentary charcoal records provide information about changes in fire regimes with, in some cases, annual and more generally multi-decadal resolution. When ap-

BGD
11, 2569–2593, 2014

propriately processed (Power et al., 2010), these records can be combined to provide composite regional or global records (see e.g. Power et al., 2008; Marlon et al., 2009; Daniau et al., 2010, 2012; Mooney et al., 2011) of glacial-interglacial changes in fire regimes. Power et al. (2008) analysed charcoal records covering the last 21 000 yr. Although regional patterns in the change in fire regimes between the Last Glacial Maximum (LGM, ca 21 000 yrs ago, 21 ka BP) and present differ, globally fire was low at the LGM and until about 16 000 yr BP, after which there was a gradual transition to the higher levels of fire characteristic of the Holocene. Daniau et al. (2012) confirmed this global pattern with an analysis of a more extensive data set, and showed that it could largely be explained in terms of changing temperature and moisture controls. Specifically, they showed that fire increased monotonically with temperature, and peaked at intermediate moisture levels. Changes in fire regime, both at a regional and global scale, tracked the glacial-interglacial increase in temperature. The strong correlation between biomass burning (indexed by charcoal abundance) and local temperature and moisture regimes obviously reflects climate controls on productivity, fuel accumulation and fuel dryness. However, the glacial-interglacial transition was also characterised by an increase in CO_2 and it is difficult to distinguish the effects of temperature increase (driven in part by rising CO_2) from the ecophysiological effects of rising CO_2 on primary production (Prentice and Harrison, 2009; Bennett et al., 2013) based on these analyses of the observations alone.

It is, however, possible to use process-based model experiments to distinguish the two effects. For example, Harrison and Prentice (2003) showed using the BIOME4 model that ecophysiological CO_2 effects are required to account for the extent of the reduction in global forest cover during glacial times. Using the same general approach and model, Bragg et al. (2013) showed that observed changes in the stable carbon isotope signature of vegetation in southern Africa are dominated by ecophysiological CO_2 effects. Prentice et al. (2011b) demonstrated that the LPX model produced realistic patterns of biome distribution at the LGM when driven by climate outputs from four coupled ocean-atmosphere general circulation models from the Palaeoclimate Modelling

BGD
11, 2569–2593, 2014

Intercomparison Project Phase 2 (PMIP2) and with the observed LGM atmospheric CO_2 level; but they did not analyse the modelled fire regimes, nor did they explicitly separate climate and CO_2 effects on vegetation.

Here, we apply the LGM climate scenarios used by Prentice et al. (2011b) to drive the LPX model (Prentice et al., 2011a). Our aim was to demonstrate whether a qualitatively realistic simulation of the patterns of biomass burning at the LGM vs. pre-industrial time could be obtained by modelling; and, if so, to assess the extent to which the well-documented increase in global biomass burning from the LGM to the Holocene could be explained by climate change alone, vs. the alternative of climate change together with the ecophysiological effects of increasing CO_2.

2 Methods

LPX (Prentice et al., 2011a) was developed from the Lund–Potsdam–Jena SPread and InTensity of FIRE (LPJ-SPITFIRE) model (Thonicke et al., 2010), which in turn was a development of the original LPJ (Sitch et al., 2003; Gerten et al., 2004) dynamic global vegetation model. LPJ simulates vegetation dynamics, and land-atmosphere exchanges of water and CO_2, using a set of nine plant functional types (PFT): tropical broadleaved evergreen tree, tropical broadleaved raingreen tree, temperate needle-leaved evergreen tree, temperate broadleaved evergreen tree, temperate broadleaved summergreen tree, boreal needleleaved evergreen tree, boreal broadleaved summergreen tree, C3 perennial grass, and C4 perennial grass. Each PFT has different dynamics in terms of production and physiological responses to climate. Photosynthetic activity depends on water availability, atmospheric concentration of CO_2 and insolation, and the net productivity accounts for carbon loss through respiration (Sitch et al., 2003).

LPJ-SPITFIRE and LPX were designed to improve on the simple representation of fire in LPJ by explicitly modelling the rate at which fire spreads as a function of physical properties (including dryness) of the fuel, and responses of the vegetation itself (including different mortality mechanisms) to the intensity and combustion efficiency of fires.

Discussion Paper | Discussion Paper | Discussion Paper | Discussion Paper |

BGD

11, 2569–2593, 2014

Climate vs. carbon dioxide controls on biomass burning

M. Martin Calvo et al.

Litter drying is calculated using a simplified form of the Nesterov Index, and fire spread follows the Rothermel equations (Rothermel, 1972). Thonicke et al. (2010) described the full set of equations and parameters in the fire component of LPJ-SPITFIRE, and Prentice et al. (2011a) documented the modifications made in LPX. Although LPJ-SPITFIRE accounts for both natural and human ignitions, lightning is the only ignition source in LPX. Only allowing natural ignitions is appropriate for palaeo-simulations when potential human ignitions are not of key importance on a global scale. LPX produces reasonable simulations of fire regimes under modern conditions, including the spatial and seasonal patterns of burnt area (Prentice et al., 2011a). Kelley et al. (2013) by quantitative comparisons against a set of benchmarks showed that both LPJ and LPX produce a good simulation of vegetation characteristics (e.g. fraction of absorbed photosynthetically active radiation, fAPAR; net primary productivity, NPP; gross primary productivity, GPP; vegetation cover; canopy height), carbon fluxes, and runoff. However, LPX produces a much better simulation of the spatial and temporal patterns of burnt area than LPJ.

We used outputs from four coupled ocean-atmosphere models: HadCM3M2, MIROC3.2, FGOALS-1.0g and CNRM-CM33 to derive LGM climate variables for LPX. The LGM simulations were run following the PMIP2 protocol (Braconnot et al., 2007), with orbital parameters for 21 ka BP, expanded ice sheets and changes in land-sea geography specified from Peltier (2004), and greenhouse gas concentrations derived from ice-core records (CO_2: 185 ppm, CH_4: 350 ppb, NO_2: 200 ppb). The control is a pre-industrial (PI: 1750 CE) simulation, with greenhouse gas concentrations corresponding to 1750 CE (CO_2: 280 ppm, CH_4: 760 ppb, N_2O: 270 ppb) and orbital parameters set to 1950 CE values (the difference in insolation patterns between 1750 and 1950 CE is negligible). Anomalies (i.e. the difference between LGM and PI gridded values) of monthly temperature, precipitation and cloudiness were bilinearly interpolated to the 0.5° grid used by LPX and then added to detrended values of these variables for the period 1900 to 1950 from the version TS 3.0 of the Climate Research Unit (CRU) data set. This results in a high-resolution LGM climate scenario, preserving inter-annual

BGD
11, 2569–2593, 2014

variability, for each model. Although several other modeling groups ran LGM simulations in PMIP2, the four selected models are representative of the range of simulated LGM climates (Harrison et al., 2013). Furthermore, Prentice et al. (2011a) have already shown that they produce a reasonably good simulation of global vegetation patterns as shown by pollen-based reconstructions.

To show the overall impact of changes in CO_2 on vegetation distribution, we use an algorithm that converts modelled vegetation properties into 12 broad vegetation types (or biomes) based on simulated canopy height, foliage projective cover, annual mean growing degree days above a baseline temperature of 5 °C, and the dominant plant functional type (Prentice et al., 2011b). We used ensemble averages of these variables for the four LGM simulations with LGM CO_2 and the four LGM simulations with pre-industrial CO_2 to derive biome maps. The pre-industrial biome distribution was simulated using the detrended CRU climate data and PI CO_2.

Charcoal data are used to provide regional indices of biomass burning. Because of the transformation necessarily involved in the processing of sedimentary charcoal records, the data cannot be interpreted in a strictly quantitative way. However, relative changes in charcoal index for a region give unambiguous information about the sign of change and an indication of the relative magnitude of changes between different intervals. Comparisons are made here between relative changes in biomass burning between LGM and PI, as modelled (with LGM CO_2 or PI CO_2), and as represented in the charcoal data assembled by Daniau et al. (2012) for the LGM and recent times. The charcoal-derived values are averages for the period from 22–20 ka BP to represent the LGM, and from 850 CE to 1750 CE for PI. The interval 22–20 ka BP is conventionally used to represent the LGM in syntheses of data (see e.g. Bartlein et al., 2011) and the PI interval was chosen to avoid major human influence on fire regimes (see e.g. Marlon et al., 2008). The charcoal-derived averages were compared to a 30 yr average of the simulated biomass burning. Relative changes were calculated as:

$$R = (X - X_{ref})/X_{ref} \qquad (1)$$

BGD
11, 2569–2593, 2014

where X is the LGM value and X_{ref} is the corresponding PI value for each latitudinal band. The latitudinal bands considered are southern extratropical (SET, > 30° S), southern tropical (ST, 0° to 30° S), northern tropical (NT, 0° to 30° N) and northern extratropical (NET, > 30° N).

Although LPX simulates the main features of modern fire regimes, there are known biases: LPX tends to underestimate burnt area in forested regions and overestimate burnt area in non-forested regions (Kelley et al., 2013). The LGM to PI transition involves large changes in the relative global coverage of forests vs. other vegetation types (Prentice et al., 2011a), and thus it was necessary to minimise these biases. This was done by classifying modelled vegetation into biomes (as described above) and then calculating the ratio of multi-annual mean burnt area within each biome from GFED3 to the multi-annual mean burnt area simulated by LPX under present climate (Table 1). We applied these ratios as correction factors to the "raw" simulated burnt area in both the PI and LGM climates. We explicitly excluded agriculture and deforestation fires from the GFED data in order to derive estimates of the natural fire regime within each biome. The ratio was calculated using the following selected regions for each of the biomes:

- Tropical forest: South America, Asia, Africa
- Temperate forest: North America, Eurasia
- Boreal forest: North America, Eurasia
- Tropical savannah: North Australia, North Africa, South Africa
- Boreal parkland: Northern Eurasia, Southern Eurasia, North America
- Dry grass/shrubland: area surrounding Aral sea, Australia, Great Basin USA
- Desert: Sahara desert, Middle East, Gobi desert
- Shrub tundra: North America, Eurasia

BGD
11, 2569–2593, 2014

– Tundra: North America, Eurasia

Warm temperate forest, sclerophyll woodland and temperate parkland were not considered for this correction because their distribution is much more restricted, and not as accurately simulated.

As a further check on the realism of the simulation of the changing terrestrial carbon cycle, simulated global carbon pools (soil and vegetation) were compared with independently estimated global values, based on ^{13}C changes from ocean sedimentary records and ice core records, for the PI (Denman et al., 2007) and LGM (Ciais et al., 2011). These estimates include an inert pool associated with permafrost. Since LPX does not simulate permafrost, our comparisons are confined to the active pool estimated by Ciais et al. (2011) and Denman et al. (2007).

3 Results

Simulated carbon pools (Fig. 1) are broadly in agreement with results presented by Ciais et al. (2011). According to the simulations, LGM carbon storage was reduced by 40–52 % (depending on the model), comparable to the 43 % reduction inferred by Ciais et al. (2011). The model results indicate that the reduction was mainly due to the ecophysiological effect of changes in CO_2 concentration, as carbon accumulation was similar to pre-industrial in the LGM simulations when CO_2 was kept unchanged at PI levels. This finding supports the suggestion of Prentice and Harrison (2009) and Prentice et al. (2011b) that an important part of the increase in carbon storage from LGM to Holocene was caused by CO_2 effects. The LGM simulations with PI CO_2 also had, on average, 88 % more of the global land area covered by forest (Fig. 2). The distribution of tropical forests, in particular, was similar to present, whereas simulations using LGM CO_2 showed a 44–45 % reduction of tropical forests, with higher levels of fragmentation – consistent with pollen records (Harrison and Prentice, 2003), and with offshore leaf-wax $\delta^{13}C$ records from tropical southern Africa (Bragg et al., 2013). Net

BGD
11, 2569–2593, 2014

primary production (NPP) was 24–27 % higher under CO_2-PI for all latitude regions, in contrast with Hickler et al. (2008), which showed bigger increases of NPP in tropical regions. This is probably due to the differences in biome distribution between present (as studied by Hickler et al.) and LGM.

Figure 3 shows the simulated changes in the carbon flux from biomass burning according to biomes. Without correction for known contemporary biases (Fig. 3, top), the modelled biomass burning flux is only modestly (8–35 %) reduced at the LGM (with realistic CO_2) relative to PI. However, bias correction (Fig. 3, middle) shows that this result is an artefact due to the greater simulated areal extent of non-forest vegetation, where the fire flux is overestimated by LPX, at the LGM. After bias correction, modelled biomass burning flux is substantially less (72–90 %) under LGM conditions. Whereas tropical forests and savannahs are major sources of CO_2 from biomass burning under recent conditions, the modelled biomass burning flux at the LGM, even after correction, is dominated by non-forest biomes (dry grass/shrublands and boreal parklands). Once the effect of biome area is eliminated (Fig. 3, bottom), the biome most affected by higher levels of CO_2 is tropical savannah but tropical forest also shows a large response to increased CO_2. These changes are consistent across climate models although there are differences in the magnitude of the changes: FGOALS-1.0g showed the biggest differences (89.9 %) in the change in tropical forests and savannahs, and MIROC3.2 the smallest (72.4 %).

The modelled effect of LGM CO_2 in suppressing biomass burning is extremely strong (Fig. 3). In the LGM climate with PI CO_2 the modelled global biomass burning flux is on average *greater* than that for the PI climate. Its distribution among biomes is similar to that in the PI climate. With LGM climate and CO_2, only 5.4 % of the flux originates in tropical forests and savannahs. With LGM climate and PI CO_2 this figure rises to 81.7 %. CO_2 concentration also has a dramatic impact on the latitudinal distribution of simulated biomass burning (Fig. 4). The southern tropics are the predominant source in the PI and still an important source in simulations with LGM climate and PI CO_2, but they play only a minor role in the simulations with LGM climate and CO_2.

BGD
11, 2569–2593, 2014

Comparisons with charcoal data (Fig. 5) indicate that the large (generally greater than PI) biomass burning fluxes modelled with LGM climate and PI CO_2, especially the consistently and greatly increased fluxes in the Northern Hemisphere, are wholly unrealistic. By contrast, the modelled biomass burning fluxes with LGM climate and CO_2 show a pattern generally consistent with the charcoal data, with realistic reductions relative to PI in the Southern Hemisphere and the northern tropics. The only exception is that three out of the four models simulate increased biomass burning at the LGM in the northern extratropics, whereas the charcoal data show a reduction in fire.

4 Discussion

Our results suggest that the ecophysiological effect of CO_2 (as opposed to climate change) on biomass burning is important, and was the dominant contribution to the observed increase in biomass burning from the LGM to the Holocene. This arises because CO_2 is the major control on net primary production, and therefore also on the amount of fuel available and the amount of carbon that returns to the atmosphere through burning. The simulated effect is strongest in the tropics, where low CO_2 dramatically reduced the area occupied by forests, and the contribution of forests and savannahs to the global biomass burning flux.

When the simulations are compared with charcoal reconstructions, the simulations with LGM climate and PI CO_2 produce unrealistic patterns, with very high burning fluxes (compared to PI) in the northern tropics and extratropics. In contrast, the simulations with LGM climate and LGM CO_2 generate a plausible latitudinal pattern of changes in biomass burning. The only exception is in the northern extratropics, where three of the individual simulations (driven by outputs from the CNRM-CM33, MIROC 3.2 and HadCM3M2 climate models) showed increases relative to PI. The PMIP models generally underestimate the magnitude of observed LGM cooling and drying in the northern extratropics (Harrison et al., 2013), leading to an unrealistically extensive simulation of forest biomes across much of the region. Indeed, the relative magnitude of the overes-

BGD
11, 2569–2593, 2014

timation in northern biomass burning is consistent with the relative underestimation of the observed cooling by the four climate models: FGOALS-1.0g produces a significant (> 8 °C) zonal cooling across northern Siberia, as does HadCM3M2, but MIROC 3.2 and CNRM-CM33 simulate marked cooling only adjacent to the European ice sheet. The PMIP2 climate models used in this study are coupled ocean–atmospheric models with prescribed vegetation, and the LGM vegetation was unchanged from the PI control simulations (see Braconnot et al., 2007). The presence of forest vegetation as the land-surface condition in the simulations, rather than the observed non-forest vegetation, may provide at least a partial explanation of the simulation of warmer-than-observed LGM temperatures across much of the northern extratropics (Harrison et al., 2013).

The LPX model (Prentice et al., 2011a) has known biases: total biomass burning fluxes are over-estimated in some non-forest biomes, and under-estimated in some forest biomes, most notably the boreal forest (Table 1). There are potentially large uncertainties in the correction factors applied here due to (a) likely direct controls of the bias by climate – the method assumes a single correction factor is appropriate regardless of climate variations within biomes, and (b) the large magnitude of the corrections for some biomes. For example, the application of a correction factor > 300 for the boreal forest could have contributed to the over-estimation of LGM fires in the northern extratropics. Nonetheless, the results presented here unambigously point to the involvement of CO_2 concentration changes in the observed major changes in global fire patterns between glacial and interglacial states of the Earth system.

The fact that fuel loads are directly affected by CO_2 changes, independent of any changes caused by changing climate, has implications for potential future changes in fire regimes. Many studies have highlighted the possibility of increased fire hazard because of climate warming (e.g. Flannigan et al., 2009); none have indicated the possibility that fire risk could increase in areas that do not experience substantial warming because the direct impact of rising CO_2 on vegetation productivity could increase fuel loads. Most projections of future fire regimes have been based on statistical modeling

BGD
11, 2569–2593, 2014

approaches (e.g. Krawchuk et al., 2009; Moritz et al., 2012), which by definition cannot account for the independent effects of changes in CO_2 on fuel loads because there is negligible (for ecophysioogical purposes) spatial variation in CO_2 concentration across the globe. However, available model-based assessments (e.g. Scholze et al., 2006; Harrison et al., 2010; Kloster et al., 2011), which in principle do take the ecophysiological CO_2 effect into account, were made using an older generation of both climate projections and vegetation-fire models. New assessments of future fire risk using more up-to-date climate scenarios and modeling tools are urgently needed.

Acknowledgements. This paper has used palaeoclimate simulations from the Palaeoclimate Modelling Intercomparison Project and modern climate data from the Climate Research Unit. We acknowledge the modeling groups participating in PMIP for providing their data for analysis, and the Laboratoire des Sciences du Climat et de l'Environnement (LSCE) for archiving the model outputs. The PMIP2 Data Archive is supported by CEA, CNRS, the EU project MOTIF (EVK2-CT-2002-00153) and the Programme National d'Etude de la Dynamique du Climat (PNEDC). Our analyses were performed using the 12/10/2006 version of the database. Pre-industrial data-model comparisons used satellite records from the Global Fire Emissions Database version 3, and palaeodata comparisons were made using raw data from the Global Charcoal Database v2.5, kindly provided by Anne-Laure Daniau, University of Bordeaux. The research leading to these results has received funding from the European Community's Seventh Framework Programme (FP7 2007-2013) under grant agreement No. 238366.

References

Aldersley, A., Murray, S. J., and Cornell, S. E.: Global and regional analysis of climate and human drivers of wildfire., Sci. Total Environ., 409, 3472–3481, doi:10.1016/j.scitotenv.2011.05.032, 2011.

Bartlein, P. J., Harrison, S. P., Brewer, S., Connor, S., Davis, B. A. S., Gajewski, K., Guiot, J., Harrison-Prentice, T. I., Henderson, A., Peyron, O., Prentice, I. C., Scholze, M., Seppä, H., Shuman, B., Sugita, S., Thompson, R. S., Viau, A. E., Williams, J., and Wu, H.: Pollen-based continental climate reconstructions at 6 and 21 ka: a global synthesis, Clim. Dynam., 37, 775–802, doi:10.1007/s00382-010-0904-1, 2011.

Bennett, J. M., Cunningham, S. C., Connelly, C. A., Clarke, R. H., Thomson, J. R., and Mac Nally, R.: The interaction between a drying climate and land use affects forest structure and above-ground carbon storage, Global Ecol. Biogeogr., 22, 1238–1247, doi:10.1111/geb.12083, 2013.

Bistinas, I., Oom, D., Sa, A., Harrison, S. P., Prentice, C. I., and Pereira, J. M. C.: Relationships between human population density and burned area at continental and global scales, PLoS One, 8, e81188, doi:10.1371/journal.pone.0081188.g001, 2013.

Bowman, D. M. J. S., Balch, J. K., Artaxo, P., Bond, W. J., Carlson, J. M., Cochrane, M. A., D'Antonio, C. M., DeFries, R. S., Doyle, J. C., Harrison, S. P., Johnston, F. H., Keeley, J. E., Krawchuk, M. A., Kull, C. A., Marston, J. B., Moritz, M. A., Prentice, I. C., Roos, C. I., Scott, A. C., Swetnam, T. W., van der Werf, G. R., and Pyne, S. J.: Fire in the Earth system, Science, 324, 481–484, doi:10.1126/science.1163886, 2009.

Braconnot, P., Otto-Bliesner, B., Harrison, S., Joussaume, S., Peterchmitt, J.-Y., Abe-Ouchi, A., Crucifix, M., Driesschaert, E., Fichefet, Th., Hewitt, C. D., Kageyama, M., Kitoh, A., Laîné, A., Loutre, M.-F., Marti, O., Merkel, U., Ramstein, G., Valdes, P., Weber, S. L., Yu, Y., and Zhao, Y.: Results of PMIP2 coupled simulations of the Mid-Holocene and Last Glacial Maximum – Part 1: experiments and large-scale features, Clim. Past, 3, 261–277, doi:10.5194/cp-3-261-2007, 2007.

Bragg, F. J., Prentice, I. C., Harrison, S. P., Eglinton, G., Foster, P. N., Rommerskirchen, F., and Rullkötter, J.: Stable isotope and modelling evidence for CO_2 as a driver of glacial–interglacial vegetation shifts in southern Africa, Biogeosciences, 10, 2001–2010, doi:10.5194/bg-10-2001-2013, 2013.

Ciais, P., Tagliabue, A., Cuntz, M., Bopp, L., Scholze, M., Hoffmann, G., Lourantou, A., Harrison, S. P., Prentice, I. C., Kelley, D. I., Koven, C., and Piao, S. L.: Large inert carbon pool in the terrestrial biosphere during the Last Glacial Maximum, Nat. Geosci., 5, 74–79, doi:10.1038/ngeo1324, 2011.

Cowling, S. A.: Plants and temperature-CO_2 Uncoupling, Science, 285, 1500–1501, doi:10.1126/science.285.5433.1500, 1999.

Dale, V. H., Joyce, L. A., Mcnulty, S., Neilson, R. P., Di, S., Ridge, O., and Box, P. O.: The interplay between climate change, forests, and disturbances, Sci. Total Environ., 262, 201–204, 2000.

Daniau, A.-L., Harrison, S. P., and Bartlein, P. J.: Fire regimes during the Last Glacial, Quaternary Sci. Rev., 29, 2918–2930, doi:10.1016/j.quascirev.2009.11.008, 2010.

Daniau, A.-L., Bartlein, P. J., Harrison, S. P., Prentice, I. C., Brewer, S., Friedlingstein, P., Harrison-Prentice, T. I., Inoue, J., Izumi, K., Marlon, J. R., Mooney, S., Power, M. J., Stevenson, J., Tinner, W., Andriè, M., Atanassova, J., Behling, H., Black, M., Blarquez, O., Brown, K. J., Carcaillet, C., Colhoun, E. A., Colombaroli, D., Davis, B. A. S., D'Costa, D., Dodson, J., Dupont, L., Eshetu, Z., Gavin, D. G., Genries, A., Haberle, S., Hallett, D. J., Hope, G., Horn, S. P., Kassa, T. G., Katamura, F., Kennedy, L. M., Kershaw, P., Krivonogov, S., Long, C., Magri, D., Marinova, E., McKenzie, G. M., Moreno, P. I., Moss, P., Neumann, F. H., Norström, E., Paitre, C., Rius, D., Roberts, N., Robinson, G. S., Sasaki, N., Scott, L., Takahara, H., Terwilliger, V., Thevenon, F., Turner, R., Valsecchi, V. G., Vannière, B., Walsh, M., Williams, N., and Zhang, Y.: Predictability of biomass burning in response to climate changes, Global Biogeochem. Cy., 26, 1–12, doi:10.1029/2011GB004249, 2012.

Denman, K. L., Brasseur, G., Chidthaisong, A., Ciais, P., Cox, P. M., Dickinson, R. E., Hauglustaine, D., Heinze, C., Holland, E., Jacob, D., Lohmann, U., Ramachandran, S., da Silva Dias, P. L., Wofsy, S. C., and Zhang, X.: Couplings between changes in the climate system and biogeochemistry, in: Climate Change 2007: The Physical Science Basis. Contribution of Working Group I to the Fourth Assessment Report of the Intergovernmental Panel on Climate Change, edited by: Solomon, S. Qin, D., Manning, M., Chen, Z., Marquis, M., Averyt, K. B., Tignor, M., and Miller, H. L., Cambridge University Press, Cambridge, UK and New York, NY, USA, 500–587, 2007.

Farquhar, G. D.: Carbon dioxide and vegetation, Science, 278, 1411, doi:10.1126/science.278.5342.1411, 1997.

Flannigan, M. D., Stocks, B. J., and Wotton, B. M.: Climate change and forest fires, Sci. Total Environ., 262, 221–9, 2000.

Flannigan, M. D., Krawchuk, M. A., de Groot, W. J., Wotton, B. M., and Gowman, L. M.: Implications of changing climate for global wildland fire, Int. J. Wildland Fire, 18, 483–507, 2009.

Franks, P. J., Adams, M. A., Amthor, J. S., Barbour, M. M., Berry, J. A., Ellsworth, D. S., Farquhar, G. D., Ghannoum, O., Lloyd, J., McDowell, N., Norby, R. J., Tissue, D. T., and von Caemmerer, S.: Sensitivity of plants to changing atmospheric CO_2 concentration: from the geological past to the next century, New Phytol., 197, 1077–1094, 2013.

Gerten, D., Schaphoff, S., Haberlandt, U., Lucht, W., and Sitch, S.: Terrestrial vegetation and water balance-hydrological evaluation of a dynamic global vegetation model, J. Hydrol., 286, 249–270, doi:10.1016/j.jhydrol.2003.09.029, 2004.

Giglio, L., Randerson, J. T., van der Werf, G. R., Kasibhatla, P. S., Collatz, G. J., Morton, D. C., and DeFries, R. S.: Assessing variability and long-term trends in burned area by merging multiple satellite fire products, Biogeosciences, 7, 1171–1186, doi:10.5194/bg-7-1171-2010, 2010.

Harrison, S. P. and Prentice, C. I.: Climate and CO_2 controls on global vegetation distribution at the last glacial maximum: analysis based on palaeovegetation data, biome modelling and palaeoclimate simulations, Glob. Change Biol., 9, 983–1004, doi:10.1046/j.1365-2486.2003.00640.x, 2003.

Harrison, S. P., Marlon, J. R., and Bartlein, P. J.: Fire in the Earth system, in: Changing Climates, Earth Systems and Society, edited by: Dodson, J., Springer Netherlands, 189–199, 2010.

Harrison, S. P., Bartlein, P. J., Brewer, S., Prentice, I. C., Boyd, M., Hessler, I., Holmgren, K., Izumi, K., and Willis, K.: Climate model benchmarking with glacial and Mid-Holocene climates, Clim. Dynam., doi:10.1007/s00382-013-1922-6, 2013.

Hickler, T., Smith, B., Prentice, I. C., Mjöfors, K., Miller, P., Arneth, A., and Sykes, M. T.: CO_2 fertilization in temperate FACE experiments not representative of boreal and tropical forests, Glob. Change Biol., 14, 1531–1542, doi:10.1111/j.1365-2486.2008.01598.x, 2008.

Kelley, D. I., Prentice, I. C., Harrison, S. P., Wang, H., Simard, M., Fisher, J. B., and Willis, K. O.: A comprehensive benchmarking system for evaluating global vegetation models, Biogeosciences, 10, 3313–3340, doi:10.5194/bg-10-3313-2013, 2013.

Kloster, S., Mahowald, N. M., Randerson, J. T., and Lawrence, P. J.: The impacts of climate, land use, and demography on fires during the 21st century simulated by CLM-CN, Biogeosciences, 9, 509–525, doi:10.5194/bg-9-509-2012, 2012.

Koch, G. W. and Mooney, H. A.: Response of terrestrial ecosystems to elevated CO_2: a synthesis and summary, in: Carbon Dioxide and Terrestrial Ecosystems, edited by: Koch, G. W. and Mooney, H. A., Academic Press, London, UK, 415–429, 1996.

Krawchuk, M. A. and Moritz, M. A.: Constraints on global fire activity vary across a resource gradient, Ecology, 92, 121–32, 2011.

Krawchuk, M. A., Moritz, M. A., Parisien, M.-A., van Dorn, J., and Hayhoe, K.: Global pyrogeography: the current and future distribution of wildfire, PLoS One, 4, e5102, doi:10.1371/journal.pone.0005102, 2009.

Krawchuk, M. A. and Moritz, M. A.: Fire regimes of China: inference from statistical comparison with the United States, Global Ecol. Biogeogr., 18, 626–639, doi:10.1111/j.1466-8238.2009.00472.x, 2009.

BGD
11, 2569–2593, 2014

Climate vs. carbon dioxide controls on biomass burning

M. Martin Calvo et al.

Los, S. O.: Analysis of trends in fused AVHRR and MODIS NDVI data for 1982–2006: indication for a CO_2 fertilization effect in global vegetation, Global Biogeochem. Cy., 27, 318–330, doi:10.1002/gbc.20027, 2013.
Marlon, J. R., Bartlein, P. J., Carcaillet, C., Gavin, D. G., Harrison, S. P., Higuera, P. E., Joos, F., Power, M. J., and Prentice, I. C.: Climate and human influences on global biomass burning over the past two millennia, Nat. Geosci., 1, 697–702, 2008.
Marlon, J. R., Bartlein, P. J., Walsh, M. K., Harrison, S. P., Brown, K. J., Edwards, M. E., Higuera, P. E., Power, M. J., Anderson, R. S., Briles, C., Brunelle, A., Carcaillet, C., Daniels, M., Hu, F. S., Lavoie, M., Long, C., Minckley, T., Richard, P. J. H., Scott, A. C., Shafer, D. S., Tinner, W., Umbanhowar, C. E., and Whitlock, C.: Wildfire responses to abrupt climate change in North America, P. Natl. Acad. Sci. USA, 106, 2519–2524, doi:10.1073/pnas.0808212106, 2009.
Mooney, S. D., Harrison, S. P., Bartlein, P. J., Daniau, A.-L., Stevenson, J., Brownlie, K. C., Buckman, S., Cupper, M., Luly, J., Black, M., Colhoun, E., D'Costa, D., Dodson, J., Haberle, S., Hope, G. S., Kershaw, P., Kenyon, C., McKenzie, M., and Williams, N.: Late Quaternary fire regimes of Australasia, Quaternary Sci. Rev., 30, 28–46, doi:10.1016/j.quascirev.2010.10.010, 2011.
Moritz, M. A., Morais, M. E., Summerell, L. A., Carlson, J. M., and Doyle, J.: Wildfires, complexity, and highly optimized tolerance, P. Natl. Acad. Sci. USA, 102, 17912–17917, doi:10.1073/pnas.0508985102, 2005.
Moritz, M. A., Parisien, M.-A., Batllori, E., Krawchuk, M. A., van Dorn, J., Ganz, D. J., and Hayhoe, K.: Climate change and disruptions to global fire activity, Ecosphere, 3, 49, 1–22, 2012.
Moritz, M. A., Hurteau, M. D., Suding, K. N., and D'Antonio, C. M.: Bounded ranges of variation as a framework for future conservation and fire management, Ann. NY Acad. Sci., 1286, 92–107, doi:10.1111/nyas.12104, 2013.
Peltier, W. R.: Global glacial isostasy and the surface of the ice-age earth: the ICE-5G (VM2) model and GRACE, Annu. Rev. Earth Planet. Sci., 32, 111–149, doi:10.1146/annurev.earth.32.082503.144359, 2004.
Power, M. J., Marlon, J., Ortiz, N., Bartlein, P. J., Harrison, S. P., Mayle, F. E., Ballouche, A., Bradshaw, R. H. W., Carcaillet, C., Cordova, C., Mooney, S., Moreno, P. I., Prentice, I. C., Thonicke, K., Tinner, W., Whitlock, C., Zhang, Y., Zhao, Y., Ali, A. A., Anderson, R. S., Beer, R., Behling, H., Briles, C., Brown, K. J., Brunelle, A., Bush, M., Camill, P., Chu, G. Q.,

Clark, J., Colombaroli, D., Connor, S., Daniau, A.-L., Daniels, M., Dodson, J., Doughty, E., Edwards, M. E., Finsinger, W., Foster, D., Frechette, J., Gaillard, M. J., Gavin, D. G., Gobet, E., Haberle, S., Hallett, D. J., Higuera, P., Hope, G., Horn, S., Inoue, J., Kaltenrieder, P., Kennedy, L., Kong, Z. C., Larsen, C., Long, C. J., Lynch, J., Lynch, E. A., McGlone, M., Meeks, S., Mensing, S., Meyer, G., Minckley, T., Mohr, J., Nelson, D. M., New, J., Newnham, R., Noti, R., Oswald, W., Pierce, J., Richard, P. J. H., Rowe, C., Sanchez-Goñi, M. F., Shuman, B. N., Takahara, H., Toney, J., Turney, C., Urrego-Sanchez, D. H., Umbanhowar, C., Vandergoes, M., Vanniere, B., Vescovi, E., Walsh, M., Wang, X., Williams, N., Wilmshurst, J., and Zhang, H.: Changes in fire regimes since the Last Glacial Maximum: an assessment based on a global synthesis and analysis of charcoal data, Clim. Dynam., 30, 887–907, doi:10.1007/s00382-007-0334-x, 2008.

Power, M. J., Marlon, J. R., Bartlein, P. J., and Harrison, S. P.: Fire history and the Global Charcoal Database: a new tool for hypothesis testing and data exploration, Palaeogeogr. Palaeoclimatol. Palaeoecol., 291, 52–59, doi:10.1016/j.palaeo.2009.09.014, 2010.

Prentice, I. C. and Harrison, S. P.: Ecosystem effects of CO_2 concentration: evidence from past climates, 5, 297–307, 2009.

Prentice, I. C., Kelley, D. I., Foster, P. N., Friedlingstein, P., Harrison, S. P., and Bartlein, P. J.: Modeling fire and the terrestrial carbon balance, Global Biogeochem. Cy., 25, 1–13, doi:10.1029/2010GB003906, 2011a.

Prentice, I. C., Harrison, S. P., and Bartlein, P. J.: Global vegetation and terrestrial carbon cycle changes after the last ice age, New Phytol., 189, 988–998, doi:10.1111/j.1469-8137.2010.03620.x, 2011b.

Rothermel, R. C.: A mathematical model for predicting fire spread in wildland fuels, USDA Forest Service, Ogden, Utah, 1972.

Scholze, M., Knorr, W., Arnell, N. W., and Prentice, I. C.: A climate change risk analysis for world ecosystems, P. Natl. Acad. Sci. USA, 103, 116–120, 2006.

Sitch, S., Smith, B., Prentice, I. C., Arneth, A., Bondeau, A., Cramer, W., Kaplan, J. O., Levis, S., Lucht, W., Sykes, M. T., Thonicke, K., and Venevsky, S.: Evaluation of ecosystem dynamics, plant geography and terrestrial carbon cycling in the LPJ dynamic global vegetation model, Glob. Change Biol., 9, 161–185, doi:10.1046/j.1365-2486.2003.00569.x, 2003.

Thompson, S. L.: Quantifying the effects of CO_2 -fertilized vegetation on future global climate and carbon dynamics, Geophys. Res. Lett., 31, L23211, doi:10.1029/2004GL021239, 2004.

Thonicke, K., Spessa, A., Prentice, I. C., Harrison, S. P., Dong, L., and Carmona-Moreno, C.: The influence of vegetation, fire spread and fire behaviour on biomass burning and trace gas emissions: results from a process-based model, Biogeosciences, 7, 1991–2011, doi:10.5194/bg-7-1991-2010, 2010.

Wang, D., Heckathorn, S. A., Wang, X., and Philpott, S. M.: A meta-analysis of plant physiological and growth responses to temperature and elevated CO_2, Oecologia, 169, 1–13, doi:10.1007/s00442-011-2172-0, 2012.

Table 1. Correction factors (rounded to two decimal places) for biomass burning, based on the ratio between GFED (non-anthropogenic) biomass burning and simulated biomass burning for each biome.

Biome	Biomass burning ratio (GFED/SIMULATIONS)
Tropical forest	3.93 ± 1.58
Temperate forest	29.92 ± 5.19
Boreal forest	373.51 ± 115.66
Tropical Savannah	0.95 ± 0.13
Boreal parkland	3.58 ± 0.87
Dry grass/shrub	0.16 ± 0.13
Desert	0.37 ± 0.23
Tundra	0.09 ± 0.03

BGD
11, 2569–2593, 2014

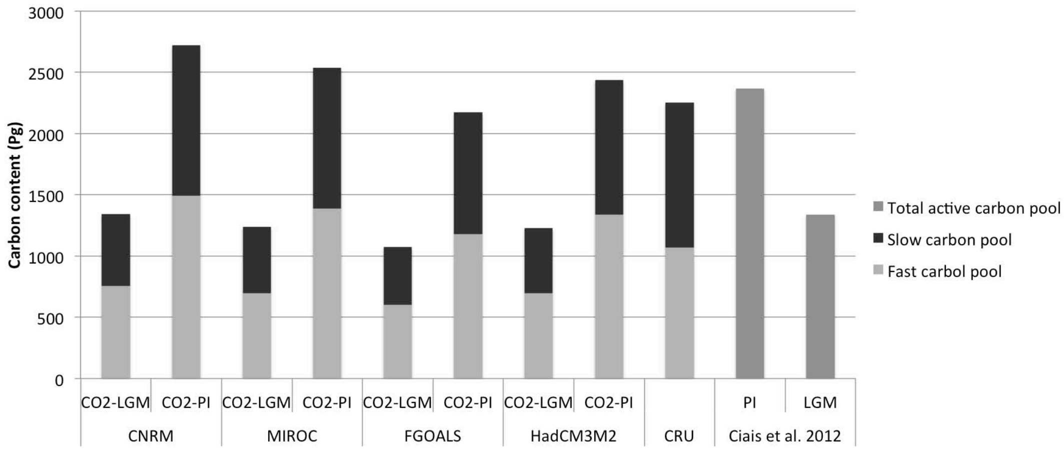

Fig. 1. Amount of carbon in the fast (cpool_fast) and slow (cpool_slow) decomposing carbon pools simulated by LPX when driven by climate outputs from the four LGM simulations and with either LGM or PI CO_2. The simulated carbon is compared to estimates of the total active pool made by Ciais et al. (2011).

BGD
11, 2569–2593, 2014

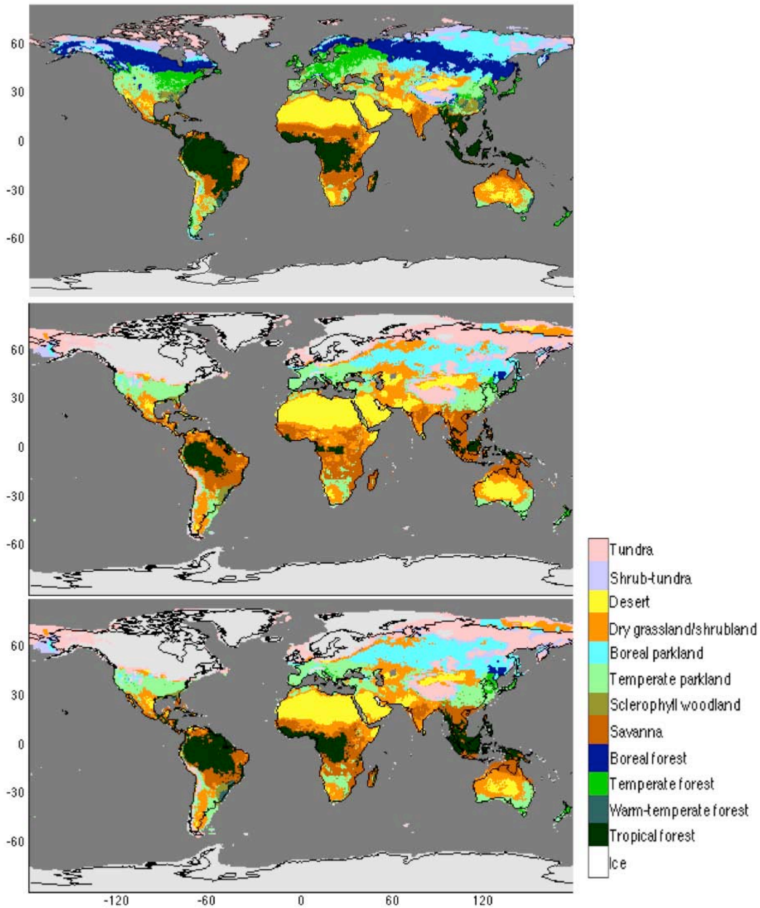

Fig. 2. Biome distributions derived from LPX simulations for PI climate and CO_2 (top), LGM climate and CO_2 (middle), and LGM climate with PI CO_2 (bottom). The LGM simulations were driven by average climate anomalies from the four scenarios.

BGD
11, 2569–2593, 2014

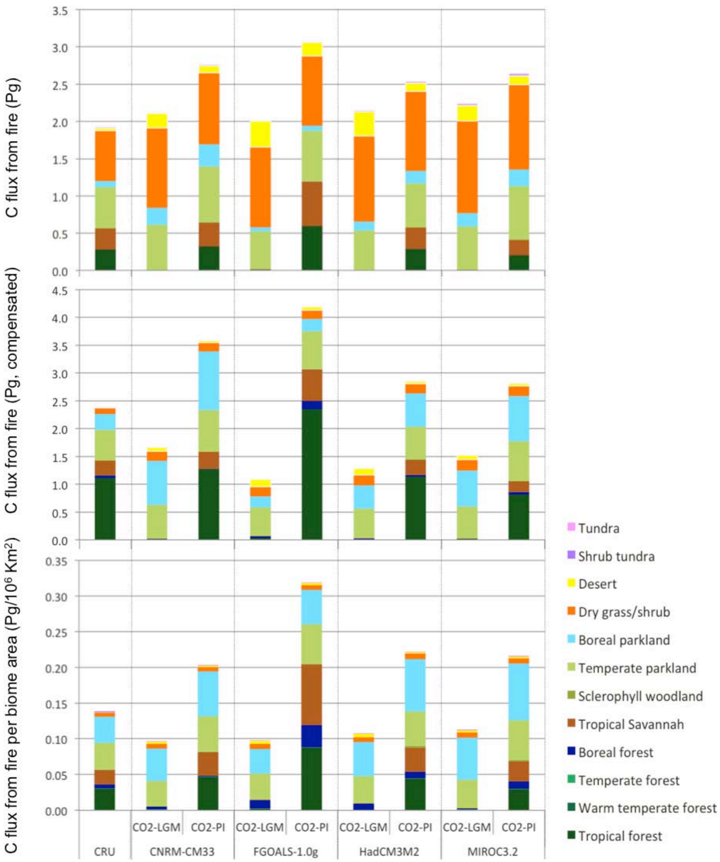

Fig. 3. Simulated carbon fluxes from fire (Pg C yr^{-1}) for each biome under PI climate and CO_2, LGM climate and CO_2, and LGM climate with PI CO_2: uncorrected results (top) and results after correction for contemporary biases (middle). To account for the differences by biome independently from the area covered by each of the biomes, the lower graph represents the biome compensated biomass burning divided by the biome area.

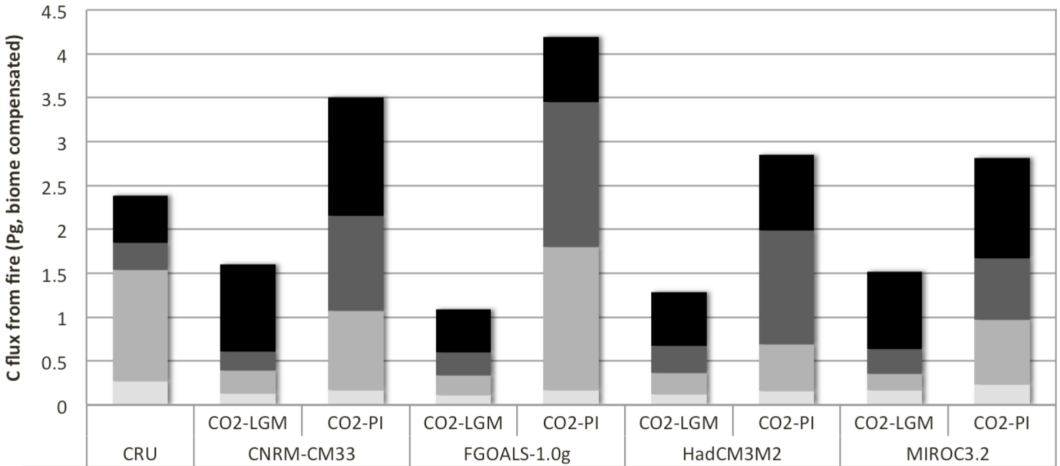

	CRU	CNRM-CM33 CO2-LGM	CNRM-CM33 CO2-PI	FGOALS-1.0g CO2-LGM	FGOALS-1.0g CO2-PI	HadCM3M2 CO2-LGM	HadCM3M2 CO2-PI	MIROC3.2 CO2-LGM	MIROC3.2 CO2-PI
NET	0.55	1.00	1.36	0.49	0.75	0.62	0.87	0.89	1.15
NT	0.30	0.22	1.08	0.27	1.65	0.30	1.29	0.28	0.70
ST	1.27	0.26	0.90	0.22	1.63	0.24	0.53	0.18	0.73
SET	0.27	0.13	0.17	0.11	0.17	0.12	0.15	0.17	0.23

Fig. 4. Simulated carbon flux from biomass burning ($Pg\,C\,a^{-1}$) by latitude bands, after applying the biome correction. The CRU column represents the PI simulation using CRU climatology, and the rest of the columns represent the values for each of the LGM climatologies and the two CO_2 scenarios. The latitude bands are Northern extra-tropics (NET, 30–70° N), Northern tropics (NT, 0–30° N), Southern tropics (ST, 0–30° S) and Southern extra-tropics (SET, 30–70° S).

BGD
11, 2569–2593, 2014

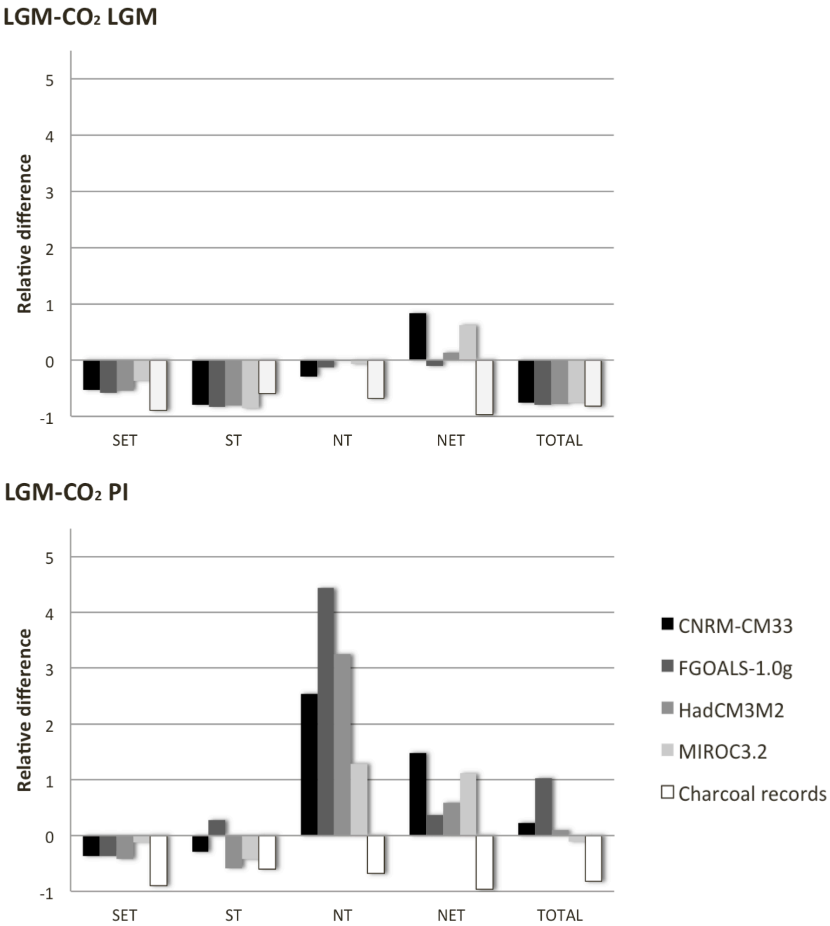

Fig. 5. Relative differences of modelled carbon flux from biomass burning by latitude bands, for LGM climate and CO_2, and LGM climate with PI CO_2, relative to PI. Relative changes in average charcoal index (from data presented in Daniau et al., 2012) are also shown.

BGD
11, 2569–2593, 2014